

THE VALIDATION OF MECHANOSTAT THEORY IN THE CASE OF PERTROCHANTERIC FRACTURES ASSISTED BY EXTERNAL FIXED IMPLANTS

Mircea DREUCEAN¹, Carmen STICLARU², Arjana DAVIDESCU³

Analiza cu element finit este utilizată pentru a studia evoluția stării de tensiune și deformație într-un femur fracturat, utilizând ca element de fixare a fracturii un implant fix. Scopul acestui studiu este de a valida teoria mechanostat în zona fracturată. Consolidarea osoasă în zona de fractură este studiată pe două tipuri de fracturi, două tipuri de implanturi pentru tipuri diferite de contacte la suprafața de contact implant - os. Concluzia acestui studiu este că stimularea consolidării osoase în zona fracturată este prezentă în cazul unei atitudini active a pacientului – mișcare, activitate zilnică.

The Finite Element Analyze is used in this paper for analyzing the evolution of stress and strain field in a fractured femur, provided with a fixed implant at the proximal end (femoral head). The purpose of the study is to validate the mechanostat theory in the fracture region. The most favourable region for bone consolidation is determined in the fracture face considering as parameters the shape of the implant on two variants and the contact type between the implant and the bone also in two variants. The conclusion of the study stresses the idea that an active attitude of a patient can stimulate the consolidation of the fractured bone, due to the stimulation of the bone growth in the fracture surface.

Keywords: FEA, Strain field, Pertrochanter fracture, Femur implant

1. Introduction

The theoretical background for this approach is provided by the mechanostat theory which proofs that the strength level in the bone is controlled by the muscles and correlated with the external loads in such a way that the strain is kept at a certain preset value. As mentioned in [2]. *H.M. Frost*, , the so called “Utah paradigm of skeletal physiology” shows how the loads on the segments of the skeleton can determine an adaptation process developed at the level of the bone cells. Other researchers [6] and [5]. *E. Schoenau*, developed this theory and studied the influence of the muscle volume and mass on the risk of

¹ Prof., Mechatronics Dept., University POLITEHNICA of Timisoara, Romania, e-mail: mircea.drecean@mec.upt.ro

² Asist. Prof., Mechatronics Dept., University POLITEHNICA of Timisoara, Romania

³ Prof., Mechatronics Dept., University POLITEHNICA of Timisoara, Romania

fracture at elder ages drawing the conclusion that “strong bones in the youngster do not automatically lead to a fracture-free old age”. They propose a new approach in the evaluation of fracture risk, based on the “functional bone-muscle unit”, taking into account the stress and the corresponding strain in the bone as a main factor in the development of the bone cell.

Frost [2] has determined two thresholds for the strain values in the bone in relation to the balance of bone loss and bone gain. The first threshold determines the start point of the bone reshaping and is detected at approx. $1500 \mu\text{Strain}$. Under this limit the process of bone loss is dominant. The second threshold is around $15000 \mu\text{Strain}$, where the fracture zone starts. Between these limits the bone gain is dominant and the bone remodelling can occur in good conditions.

The target of this paper is to determine the strain level in a fracture area of a femoral head (petrochanteric fracture type 31 A1 conforming to [1]) assisted by an external fixed implant in two design variants. The shape of the implants is presented in Fig. 1 and Fig. 2. The strain level can indicate the zone where the bone remodelling is stimulated by the strain values.

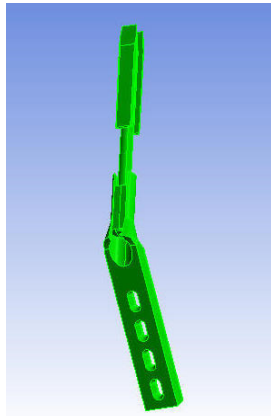


Fig. 1. External fixed implant with rotated H orientation for higher rigidity



Fig. 2. External fixed implant with regular H orientation for normal rigidity

The models for the FEA were created using two different contact types for the bone-implant boundary: “bonded” was the first option and “no separation” was the second option. In many papers dealing with FEA of implanted bones the authors use bonded contact between bone and implant, considering that the implant should be “bonded” with the bone after the Osseo integration period. That is acceptable for a certain extent, but in the first days after implantation this assumption is not correct and we consider that the best contact model is “no separation”. Another initial condition of the model is the separation of the

femoral head in 6 different regions with specific elastic properties, according to the theory of [3]. *R.H.Gahr, K.S.Leung, M.P Rosenwasser, W.Roth*

2. FEM Model

The load model takes into consideration the results of many researchers who studied the transfer of forces and torque between the pelvis and the femur head during the gait phases. [4]. *F. Pauwels*, . The load consists of a reduced force applied on the femoral head, as coming from the acetabular cap. (see Fig.3). The load components along the axis are $X = -1060.1$ N, $Y = 0$ N and $Z = 2913.1$ N. The Z axis is oriented along the femur from proximal to distal end. The resultant force on the femoral head is 3100 N. The orientation of the load is defined according to ISO 7206-4:2010. In sagittal plane the force vector is 16° tilted towards the bone and 16° tilted from the middle plane in the lower-back lateral direction.



Fig. 3. Oblique load at the proximal end of the femur and total constraint (fixed support) at the distal end

The femur head, neck and trochanter is considered to be non homogeneous, with a structure consisting of 6 different regions. The regions are distinct in shape and volume and in bone density and Young modulus (table 1). All the distinct regions are considered bounded from the point of view of the FEA.

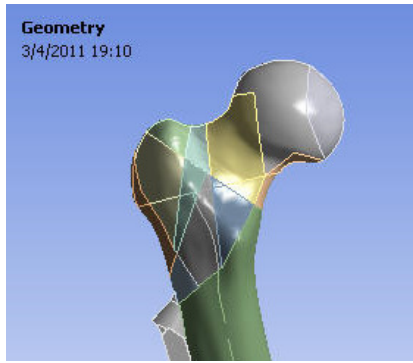


Fig. 4. Distinct regions of the proximal end of the femur

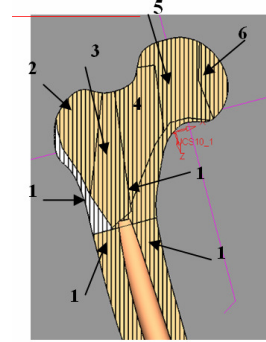


Fig. 5. Representation of the proximal end with distinct regions

Table 1
The relative values of Young modulus for different regions of the proximal end of femur

Femoral proximal end region	1	2	3	4	5	6
$\frac{E_{\text{cortex}}}{E_{\text{cancellous}}}$	1	10	12	15	30	20

Bone material shows an anisotropic material behaviour. In order to consider the non-homogeneity of the cancellous bone, the corresponding finite element model was split into subzones, each of which had different material properties ([3]. R.H.Gahr, K.S.Leung, M.P Rosenwasser., W.Roth). In table 2 the values for the different regions of the femur are presented; the Poisson's ratio is 0.3 for all cases. In the table 3 the titanium alloy properties (used for the implant) are presented.

Table 2
The absolute values of Young modulus for different regions of the proximal end of femur

Femoral head region	1	2	3	4	5	6
E [MPa]	14500	1450	1210	970	485	725

Table 3

The properties for the titanium alloy (TiAl6V4)

Structural	
Young's Modulus	96000 MPa
Poisson's Ratio	0,36
Density	4,62e-006 kg/mm ³
Thermal Expansion	9,4e-006 1/°C
Tensile Yield Strength	930, MPa

Compressive Yield Strength	930, MPa
Tensile Ultimate Strength	1070, MPa
Compressive Ultimate Strength	0, MPa
Thermal	
Thermal Conductivity	2,19e-002 W/mm·°C
Specific Heat	522, J/kg·°C
Electromagnetics	
Relative Permeability	10000
Resistivity	1,7e-003 Ohm·mm

3. Results

The simulation followed two directions: to point out the influence of the implant design on the equivalent strain in the fracture plane and the influence of the contact type between bone and implant on the equivalent strain in the same region. The contact type is relevant only from the point of view of the simulation, because in reality, for the first stage, the contact type between stem and bone is “no separation”. In the initial stage after implantation, there is no osseointegration and the implant may slide gently inside the bone structure. In this way the deformation of the implant under the loads can be different from the deformation of the bone. After the osseointegration process, when the implant is well fixed in the bone, the most appropriate contact model is “bonded”. The deformation of the implant and the bone in the contact area are identical and no sliding is possible. The fracture plane is presented in Fig. 6.

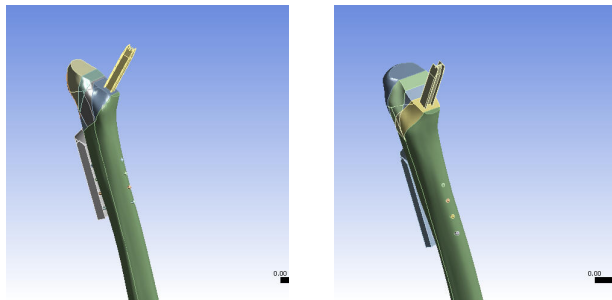


Fig. 6. The fracture plane- pertrochanteric fracture type 31 A1 for the two types of implants

The first analysis was run for the implant presented Fig. 1. The limits for equivalent von-Mises strain in the fracture area are between 15104 μ Strain and 169 μ Strain for contact type “bonded” (see Fig. 7).

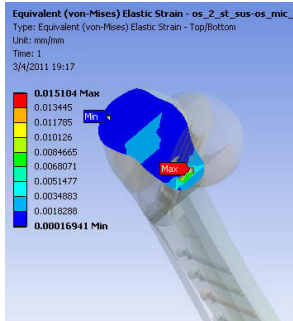


Fig. 7. The equivalent strain for rotated H implant and bonded contact

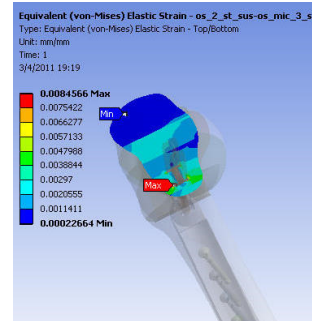


Fig. 8. The equivalent strain for rotated H implant and no separation contact

For the same type of implant but “no separation” contact the limits are between 8456 μ Strain and 226 μ Strain (see Fig. 8). Considering the values from the simulation, one can see that in the first case, (Fig. 7), the maximum value exceeds the mechanostat upper limit and the minimum value is much under the mechanostat lower limit. Therefore the bone reshaping condition is met only in a small region of the smaller trochanter, on the contracted zone of the bone. All the greater trochanter area is under the mechanostat limit and no bone reshaping can occur in that region. In the second case, (Fig. 8), the maximum value is closer to the upper limit of the mechanostat condition and the minimum value is very low. The dark blue area of the representation is smaller than in the first case and the consequence is that the bone reshaping condition is met in a wider extent for this case. The favourable zone for this effect is again the compressed line of the smaller trochanter.

The second analysis was run for the implant presented in Fig. 2. The limits for equivalent von-Mises strain in the fracture area are between 12208 μ Strain and 70.73 μ Strain for contact type “bonded” (see Fig. 9).

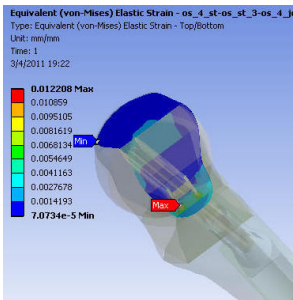


Fig. 9. The equivalent strain for regular H implant and bonded contact

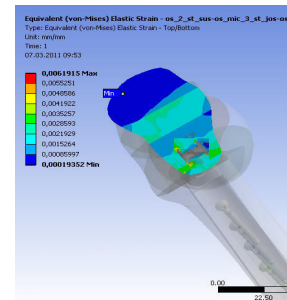


Fig. 10. The equivalent strain for regular H implant and no separation contact

For the same type of implant but “no separation” contact, the limits are between 6191 μ Strain and 193 μ Strain (see Fig. 10). Considering the values in this second analyse, the maximum value for bonded contact exceeds the mechanostat upper limit and the minimum value is very low, much under the mechanostat lower limit. The distribution of strain in the fracture surface is more favourable comparing with the rotated H implant, and extends also towards the greater trochanter. The most favourable zone is the compressed bone under the implant in the smaller trochanter area, similar to the first studied implant. A good part of the greater trochanter area is under the mechanostat limit and no bone reshaping can occur in that region. For the second situation of contact, no separation, (Fig. 10), the maximum value is within the limits of mechanostat condition and the minimum value is out of the interval. The dark blue area of the representation is smallest from all the presented situations and the consequence is that the bone reshaping condition is met in the widest extent for this case. The favourable zone for this effect is again the compressed line of the smaller trochanter.

For both type of implants the mechanostat conditions are met in the surface of the fracture in a zone around the implant. This zone is larger for the regular H implant and smaller in the other case for the rotated H implant. The light green zone represents in both cases the area with mechanostat conditions fulfilled. The maximum value of strain for both types of implants over draw very much over the limits of the bone reshaping values and in that situation small cracks can occur in the bone and bone growth is compromised. That happens in general in the compressed area of the femoral neck in the case of pectrochanteric fracture.

The contact type considered in the simulation has a good influence on the results, showing for both types of implants a reduce in maximum values of strain for the “no separation” contact as an effect of the more independent deformation of the bone. Also the area of distribution of mechanostat conditions in the surface of the fracture is larger in the case of “no separation” contact.

4. Conclusions

Analyzing the results of this study one can reveal the importance of the bone reshaping conditions that occur in the fracture surface for the healing process of a real patient. The loads applied on the fracture surface are a condition of reshaping the bone according to the mechanostat theory and these loads are applied only if the patient has an active attitude during the healing process. A constant load applied on the implanted femur is a good guarantee of the rapid healing.

The future studies should be oriented to the implant design in order to stimulate the distribution of stress and strain in the fracture surface on the purpose to enlarge the area with mechanostat conditions.

It could be also relevant to study other types of implants and other situations of fractures to see how the bone reshaping conditions are met for different situations.

An experimental validation of this simulation study is also needed for a better understanding of the healing process.

R E F E R E N C E S

- [1]. *** <http://www.aofoundation.org> accessed on the 04.03.2011
- [2]. *H.M . Frost*, The Utah paradigm of skeletal physiology: an overview of its insights for bone, cartilage and collagenous tissue organs, in *Journal of Bone and Mineral Metabolism*, **18(6)**:305–316, 2000.
- [3]. *R.H.Gahr, K.S.Leung, M.P Rosenwasser, W.Roth* The Gamma Locking Nail, Einhorn-Press Verlag GmbH Reinbek, ISBN 3- 88756-808-7, 1999.
- [4]. *F. Pauwels*, Biomechanics of the Locomotor Apparatus. Springer Verlag, New York, pp 1-228, 1980.
- [5]. *E. Schoenau*, From mechanostat theory to development of the "Functional Muscle-Bone-Unit", in *Journal of Musculoskeletal Neuronal Interact*; **5(3)**:232-238, 2005.
- [6]. *E . Schoenau, C.M. Neu, B. Beck, F. Manz, F. Rauch*, Bone Mineral content per Muscle Cross-Sectional Area as an Index of the Functional Muscle-Bone Unit, in *Journal of Bone and Mineral Research*, **Vol.17**, S.1095-1101, 2002.